GMR
The Original

COMPUTATIONAL SCREENING OF PHYTOCHEMICAL–CHITOSAN NANO-CONJUGATES AGAINST WHO-PRIORITY PATHOGENS IN CONTAMINATED FRESHWATER ECOSYSTEMS

P. Ananthakrishnan[1], G.Gayathri[2]*, A.K.Kathireshan[3]

[1,2,3] Department of Microbiology, School of Life Sciences, Vels Institute of Science, Technology and Advanced Studies (VISTAS)

ABSTRACT
Urban freshwater lakes, including those in rapidly growing cities like Chennai, act as important environmental reservoirs for antibiotic-resistant bacteria, driven largely by anthropogenic pollution and wastewater inputs. In this computational study, we synthesized published data on bacterial communities from Chennai lake water, with emphasis on two high-priority WHO pathogens: carbapenem-resistant Pseudomonas aeruginosa and methicillin-resistant Staphylococcus aureus. Resistance gene profiles were characterized through literature mining and visualized using Python libraries (Pandas, Matplotlib, Seaborn), highlighting dominant mechanisms including efflux pumps, enzymatic inactivation, and target-site alterations. Blind molecular docking simulations (CB-Dock2) assessed the binding potential of key phytochemicals isolated from Caesalpinia sappan—brazilin, brazilein, sappanchalcone, caesalpinin, and cholic acid—both alone and conjugated with chitosan nanoparticles, targeting the aminoglycoside-modifying enzyme Aac(6′)-Ib (PDB ID: 2QIR). Results demonstrated that chitosan conjugation markedly improved binding affinities for all tested ligands, with the most pronounced enhancements observed for brazilein (from −9.1 to −14.8 kcal/mol) and cholic acid (from −9.3 to −14.7 kcal/mol). These in silico findings indicate that C. sappan-derived compounds, particularly when combined with chitosan, may offer promising natural scaffolds for inhibiting resistance enzymes in contaminated aquatic systems. The work underscores the value of computational approaches in exploring sustainable bioremediation options while emphasizing the essential need for subsequent experimental confirmation, including in vitro assays and molecular dynamics simulations, to combat antimicrobial resistance in polluted freshwater environments.

KEYWORDS: Chennai lake water, antibiotic resistance, Pseudomonas, Staphylococcus, bioremediation, molecular docking, phytochemicals, chitosan nanoparticles

INTRODUCTION

Lakes serve as critical freshwater reservoirs, supporting biodiversity and human activities. However, increasing urbanization and anthropogenic activities have led to the contamination of these water bodies with various pollutants, including antibiotics. Chennai's lakes, in particular, face significant environmental stress, yet studies on their bacterial communities remain limited. While some research has explored bacterial diversity in soil, such as the study on the Madras Christian College campus, a comprehensive analysis of pathogenic bacteria in Chennai's lakes is still lacking. This study aims to fill this gap by characterizing antibiotic-resistant bacterial species in Chennai's lake water samples and identifying potential bioremediation agents [1].

The contamination of freshwater bodies with antibiotics is a growing concern, as it accelerates the development of antimicrobial resistance (AMR) in bacterial communities. Antibiotic residues often enter water bodies through industrial discharge, agricultural runoff, and untreated sewage, creating an environment where bacteria can evolve resistance mechanisms. Pathogenic bacteria such as Pseudomonas and Staphylococcus are known to thrive in such conditions, posing potential health risks to communities relying on these water sources for daily activities. Understanding the genetic basis of antibiotic resistance in these pathogens is essential for developing effective mitigation strategies [2, 3].

While previous studies have investigated bacterial diversity in different ecological niches of Chennai, research specific to lake water remains scarce. Given the city's rapid expansion and increasing pollution levels, it is crucial to assess the bacterial composition and resistance profiles of its freshwater sources. Identifying resistance genes in lake water samples will not only provide insights into environmental AMR trends but also inform public health interventions aimed at controlling the spread of resistant pathogens. Furthermore, exploring novel bioremediation strategies, such as phytochemicals and nanoparticles, may offer sustainable solutions for reducing antibiotic contamination [4, 5].

In this study, we employ a multi-disciplinary approach that combines genomic, transcriptomic, and molecular docking analyses to investigate antibiotic-resistant bacteria in Chennai's lakes. By characterizing the resistance genes present in Pseudomonas and Staphylococcus, we aim to elucidate the molecular mechanisms driving AMR in these environments. Additionally, we evaluate the potential of Caesalpinia sappan extracts and chitosan nanoparticles as bioremediation agents, which could contribute to future efforts in controlling the spread of antibiotic resistance in freshwater ecosystems. This study aims to bridge this gap by characterizing antibiotic-resistant bacterial species in Chennai's lake water samples. Through genomic and transcriptomic analyses,

MATERIALS AND METHODS

1. Bacterial Identification: Various research studies have been analyzed to conclude the presence of bacterial sample present in the lake water of Chennai. In these studies, water samples were collected from multiple locations across Chennai's lakes to ensure a representative analysis. Based on this analysis various bacteria have been found in the lakes of Chennai. Based on further analysis of risk percentage in humans, two bacteria were selected, *Pseudomonas* aeruginosa *and Staphylococcus aureus*. All these analyses have been done using python programming language [6, 7, 10, 11].

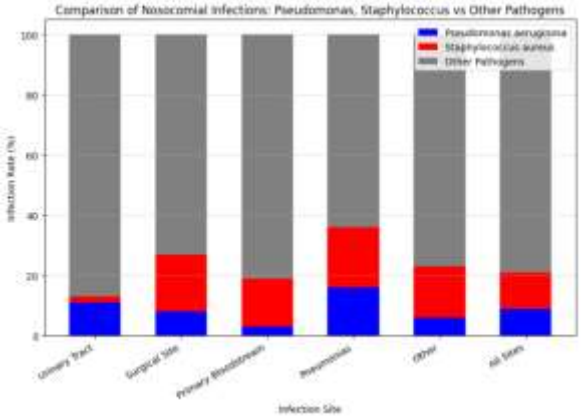

Figure 1: Distribution of nosocomial infections caused by *Pseudomonas aeruginosa* (blue), *Staphylococcus aureus* (red), and other pathogens (grey) across various infection sites

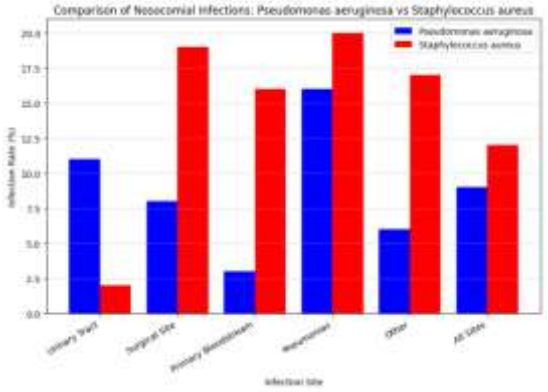

Figure 2: Comparative infection rates of *Pseudomonas aeruginosa* (blue) and *Staphylococcus aureus* (red) at different nosocomial infection sites.

The data for these two graphs has been adapted from the research of the **University of Texas Medical Branch at Galveston** [8]**.**

This analysis compares *Pseudomonas aeruginosa*, *Staphylococcus aureus*, and all other nosocomial pathogens across various infection sites. *Pseudomonas aeruginosa* contributes significantly to pneumonias (16%) and urinary tract infections (11%). *Staphylococcus aureus* is a major cause of surgical site infections (19%), bloodstream infections (16%), and pneumonias (20%). Other pathogens collectively account for the majority of infections across all sites, indicating the broad diversity of hospital-acquired infections.This highlights the need for broad-spectrum infection control measures, particularly against resistant strains such as *Pseudomonas aeruginosa* and MRSA (*Methicillin-resistant Staphylococcus aureus*) [8]**.**

2. Resistance Gene Analysis: Further referring to the data of WHO , it has been found that Pseudomonas aeruginosa and Staphylococcus aureus are the antibiotic resistant and there is urgent need to find new antibiotic for these two, as *Pseudomonas* aeruginosa *(*carbapenem-resistant *)* is in the *"*Priority 1: CRITICAL" list of WHO and *Staphylococcus aureus* (methicillin-resistant, vancomycin-intermediate and resistant) is in the *"*Priority 2: HIGH" list of WHO.

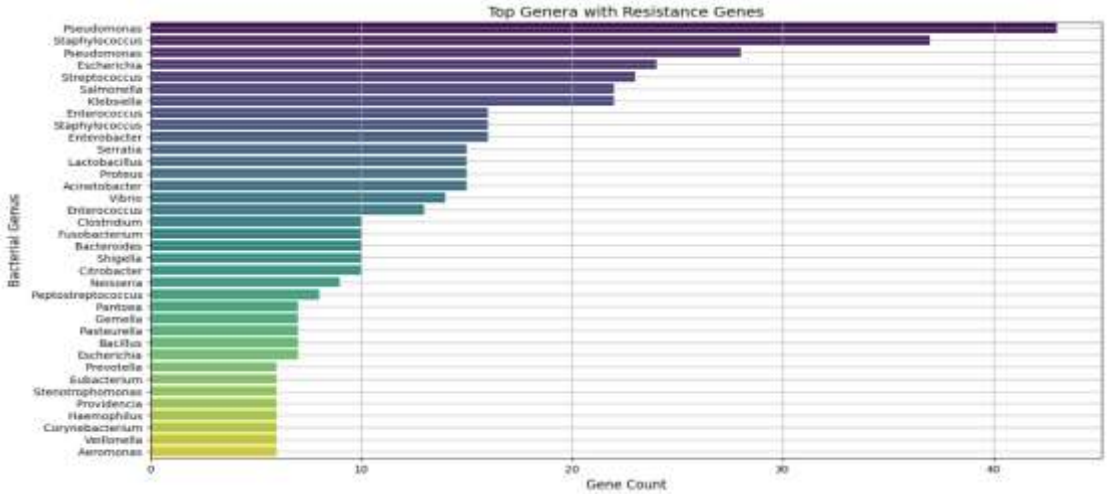

Figure 3: Top Genera with Resistance genes

Resistance genes were classified based on their involvement in antibiotic modification, efflux pump activity, and target site modification. The dataset used for this analysis was obtained from van Hoek et al. (2011). Python-based statistical and visualization tools were used to identify significant resistance markers [9, 10, 11].

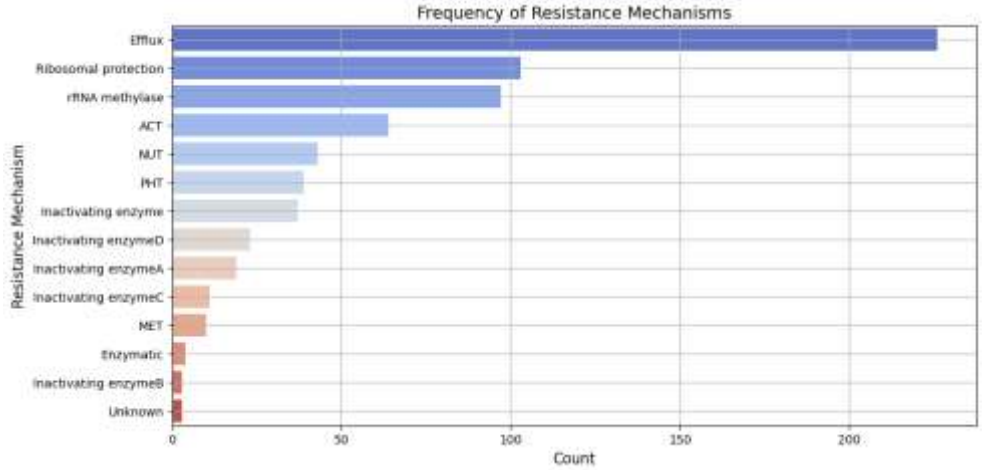

Figure 4: Frequency of resistance mechanisms

The bar chart illustrates the frequency of various antibiotic resistance mechanisms. Efflux pumps dominate as the most prevalent mechanism, followed by ribosomal protection and rRNA methylation. Other mechanisms, such as enzymatic inactivation and modification of target sites (e.g., ACT, NUT, and PHT), are also observed but at lower frequencies. The presence of multiple inactivating enzymes suggests diverse adaptive strategies employed by bacteria to counteract antibiotics [9, 10, 11].

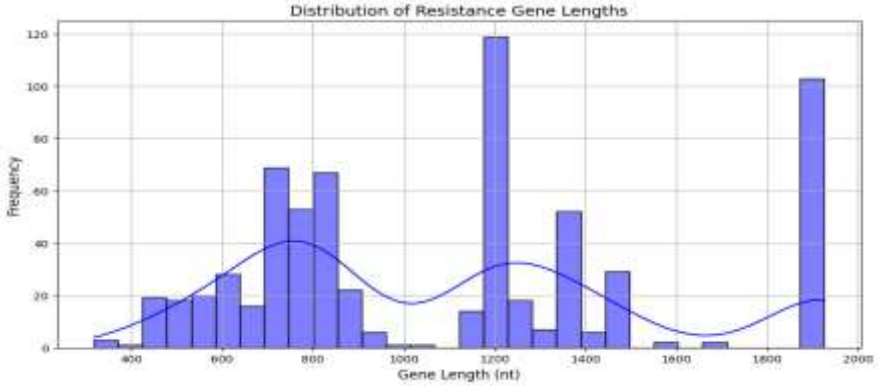

Figure 5: Distribution of Resistance Gene Lengths

The histogram represents the distribution of resistance gene lengths, highlighting multiple peaks, indicating a diverse range of gene sizes. Notably, genes of approximately 800 nt, 1200 nt, and 1900 nt are most frequently

observed, suggesting common resistance-associated gene lengths. The kernel density estimate (KDE) further emphasizes the multimodal distribution pattern, indicating variations in gene size distributions across different resistance determinants [9, 10, 11]. For the data analysis various libraries of python has been used. Some of them are Pandas, numpy, matplotlib, and seaborn. All the graphs has been plotted using matplotlib and seaborn [15, 16, 17, 18].

3. Molecular Docking: Molecular docking was performed using **CB-Dock2** to evaluate the binding efficacy of phytochemical extracts from *Caesalpinia sappan* and chitosan nanoparticles against the identified resistance proteins. The docking studies targeted **Aac(6')-Ib** (PDB ID: 2QIR), a key aminoglycoside resistance enzyme [12, 13, 14]. This gene has been selected based on data of van Hoek et al. (2011). For preparing the ligands for docking, PyMol has been utilized. PyMOL is an open-source molecular visualization tool widely used in structural biology, bioinformatics, and drug discovery [19, 20].

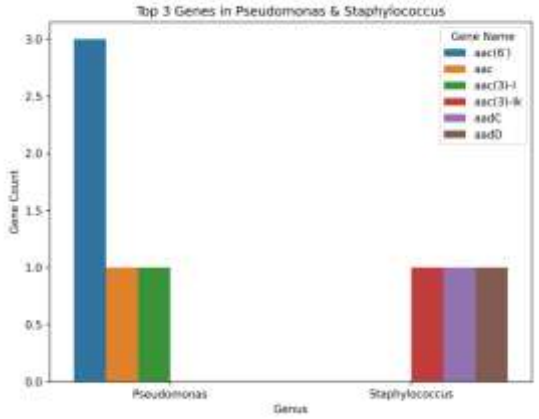

Figure 6: Top genes in Pseudomonas and Staphylococcus

Table 1: The phytochemicals

Phytochemical	PubChem CID	Combined with	PubChem CID
Brazilin	73384	Chitosan	71853
Brazilein	6453902	Chitosan	71853
Sappanchalcone	5319493	Chitosan	71853
Caesalpinin	11419457	Chitosan	71853
Cholic Acid	221493	Chitosan	71853

Docking interactions were analyzed based on binding affinity and stability, with a focus on inhibitory potential against resistance proteins.

RESULTS AND DISCUSSION

Bacterial Diversity, Resistance Gene Patterns and Resistance Mechanisms

Analysis of Chennai's lake water revealed the presence of multiple pathogenic bacterial species, with *Pseudomonas aeruginosa* and *Staphylococcus aureus* being the most dominant. Other bacteria identified include *Klebsiella pneumoniae*, *Serratia marcescens*, *Enterobacter cloacae*, *Bacillus cereus*, *Streptomyces*, and *Clostridium*. The classification of these bacterial species aligns with previous studies. The resistance gene analysis showed that *Pseudomonas* exhibits strong resistance through efflux pumps and enzymatic degradation mechanisms, particularly against aminoglycosides and beta-lactams. In contrast, *Staphylococcus* resistance was primarily associated with ribosomal protection and target site modification. These findings align with WHO's priority list of antibiotic-resistant pathogens, which highlights *Pseudomonas aeruginosa* and *Staphylococcus aureus* as critical and high-priority threats.

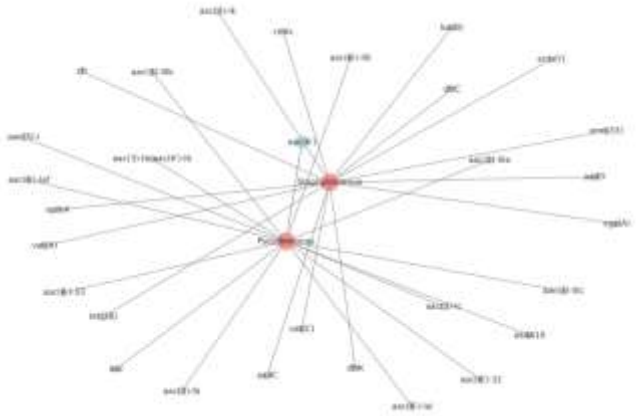

Figure 7: Network Graph showing resistant genes

Highly connected nodes (hubs) such as *aac(6')-Ib*, *aph(3')-IIIa*, and *blaOXA* suggest these genes play a crucial role in resistance across multiple isolates. *Pseudomonas* has a denser network, indicating strong gene clustering, particularly among beta-lactamases and efflux-related genes. *Staphylococcus* shows a more diverse but less interconnected network, suggesting multiple independent resistance pathways. The force-directed layout helps in distinguishing highly associated genes, which could be potential targets for future antimicrobial strategies.

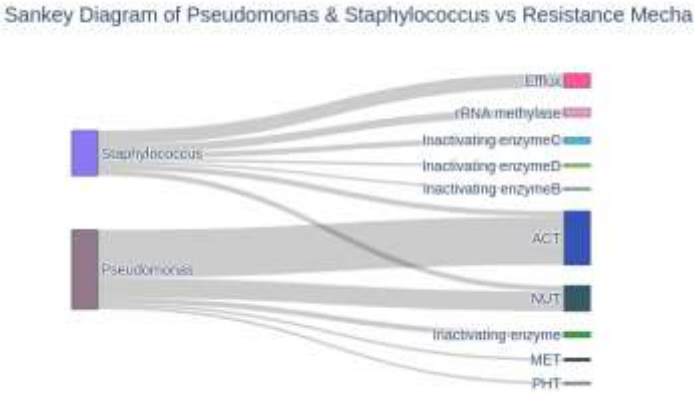

Figure 8: Sankey Plot showing top resistant genes

Pseudomonas predominantly exhibits resistance through **efflux pumps and enzymatic degradation**, showing a strong correlation with genes involved in aminoglycoside and beta-lactam resistance. *Staphylococcus* resistance is more evenly distributed across **ribosomal protection and target site modification**, indicating a different adaptation strategy against antibiotics.

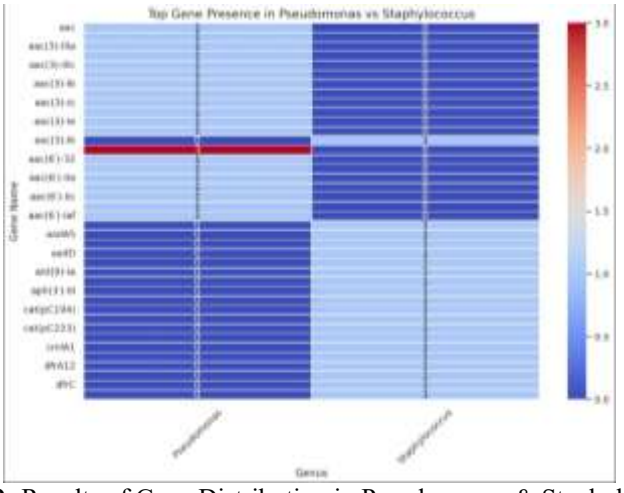

Figure 9: Results of Gene Distribution in Pseudomonas & Staphylococcus

The heatmap illustrates the distribution of resistance genes across *Pseudomonas* and *Staphylococcus*. Some genes are exclusive to one genus, while others are shared between both. *Pseudomonas* resistance is dominated by aac(6′) and aac(3)-related genes, emphasizing aminoglycoside resistance. *Staphylococcus* exhibits a broader gene distribution, including *aadA5* and *aph(3′)-III*, indicating diverse resistance mechanisms. No single gene is highly dominant, suggesting the presence of multiple resistance mechanisms within each genus.

Table 2: Most frequent genes in Pseudomonas & Staphylococcus

Genera	Most frequent genes
Pseudomonas	*aac(6')*, *aac(3)-IIIa*, *aac(3)-Ib*, *aac(3)-IIIb*. These genes are primarily associated with aminoglycoside resistance.
Staphylococcus	*aac(3)-Ik*, *aph(3')-III*, *aadD*, *apmA*. These genes are involved in antibiotic modification and resistance mechanisms.

Molecular Docking

The docking results revealed strong binding interactions between resistance proteins and the tested phytochemicals. These findings suggest that *Caesalpinia sappan* extracts and chitosan nanoparticles could serve as potential bioremediation agents for targeting antibiotic resistance in aquatic environments.

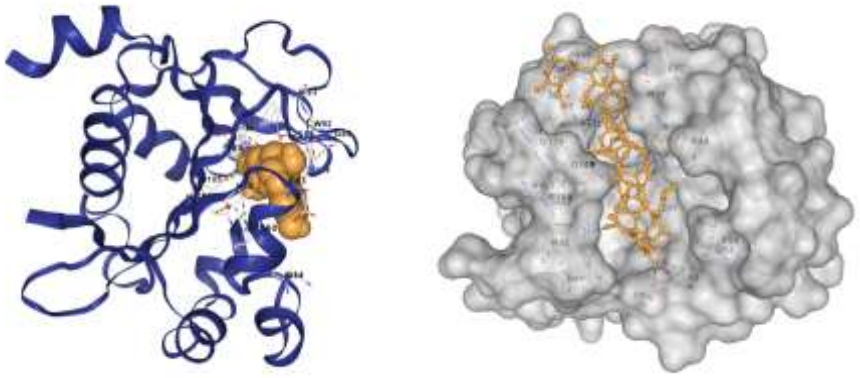

Figure 10: (a) Docked figure of Brazilin with 2QIR (b) Docked figure of Brazilin in conjugation with chitosan with 2QIR

Table 3: Docking scores for Brazilin with and without Chitosan

CurPocket ID	Vina Score (Without Chitosan)	Vina Score (With Chitosan)	Cavity Volume (Å³)	Center (x, y, z)	Docking Size (x, y, z)
C3	-9.3	-8.6	153	14, 17, -12	20, 20, 20 (without) / 42, 42, 42 (with)
C1	-9.0	-10.8	771	3, 9, -20	20, 20, 20 (without) / 42, 42, 42 (with)
C5	-8.4	-10.6	65	13, 7, -13	20, 20, 20 (without) / 42, 42, 42 (with)
C4	-7.4	**-11.1**	123	22, 12, -17	20, 20, 20 (without) / 42, 42, 42 (with)
C2	-5.5	-8.7	712	10, 15, -34	20, 20, 20 (without) / 42, 42, 42 (with)

The best docking score improved from **-9.3 to -11.1** upon adding Chitosan (C4). All binding pockets showed an overall increase in binding affinity with Chitosan. The docking box size increased from **20×20×20** to **42×42×42**, indicating a broader search space. The improved scores suggest stronger interactions and enhanced binding stability due to Chitosan.

Table 4: Interacting Residues for Brazilin

Pocket ID	Score	Interacting Residues (Chain A)
C3 (without chitosan)	-9.3	TRP39, GLN54, TYR55, LEU60, GLU63, VAL65, TYR79, GLN81, TYR83, VAL84, ALA85, GLY87, SER88, GLY89, ASP90, TRP92, TRP93, ILE104, ASP105, GLN140, ASP142, ASP169

C4 (with chitosan)	-11.1	VAL36, GLU37, TRP38, TRP39, ALA44, PRO46, ASP50, GLN54, TYR55, LEU60, GLU63, VAL65, GLN81, TYR83, SER88, GLY89, ASP90, GLY91, TRP92, TRP93, GLU94, GLU95, GLU96, ASP105, GLN106, GLN140, ASP142, PRO143, SER144, PRO145, SER146, ASN147, LEU148, ALA150, ILE151, ARG161, GLN162, GLY163, THR164, VAL165, THR166, THR167, PRO168, ASP169, GLY170, PRO171, ALA172, VAL173, TYR174

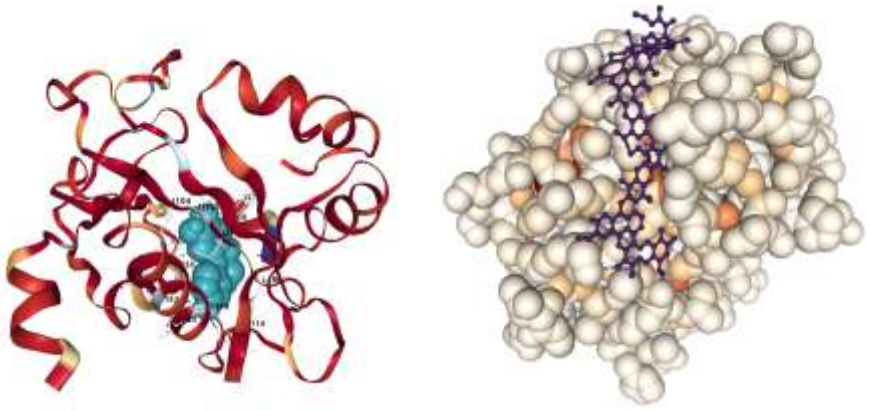

Figure 11: (a) Docked figure of Brazilein with 2QIR (b) Docked figure of Brazilein in conjugation with chitosan with 2QIR

Table 5: Docking scores for Brazilein with and without Chitosan

CurPocket ID	Vina Score (Without Chitosan)	Vina Score (With Chitosan)	Cavity Volume (Å³)	Center (x, y, z)	Docking Size (x, y, z)
C1	-9.1	-12.9	771	3, 9, -20	20, 20, 20(without) / 37, 37, 37
C3	-8.7	-14.3	153	14, 17, -12	20, 20, 20(without) / 37, 37, 37
C5	-8.1	-14.0	65	13, 7, -13	20, 20, 20(without) / 37, 37, 37
C4	-7.6	-14.7	123	22, 12, -17	20, 20, 20(without) / 37, 37, 37
C2	-5.3	-14.8	712	10, 15, -34	20, 20, 20(without) / 37, 37, 37

The vina scores significantly improved (more negative) with chitosan, indicating stronger binding. The docking size increased from **20×20×20** to **37×37×37** after adding chitosan. The best docking score was observed for **C2 (-14.8) with chitosan**, compared to **C1 (-9.1) without chitosan**. The order of the best binding pockets also changed, with **C2 ranking highest after chitosan addition**.

Table 6: Interacting Residues for Brazilein

Pocket ID	Score	Interacting Residues (Chain A)
C2(with chitosan)	-14.8	SER12, VAL13, THR14, LEU15, VAL101, LYS121, ARG124, ALA125, LEU126, GLU128, LEU129, ASN132, THR137, LYS138, ARG152, GLU155, LYS156, ALA157, GLY158, PHE159, GLU160, ARG161, GLN162, GLY163, TYR174, VAL176, THR178, GLN180, ALA181, PHE182, ARG184, THR185, ARG186, SER187
C1(without chitosan)	-9.1	HIS34, ILE35, VAL36, GLU37, TRP38, TRP39, TYR55, GLN81, TRP92, ILE104, ASP105, GLN106, LEU107, LEU108, ALA109, LEU114, GLY115, LEU118, GLY119, THR120, ASP142, PRO143, SER144, SER146, ASN147, ARG149, ALA150, ILE151, CYS153, TYR154, ASP169

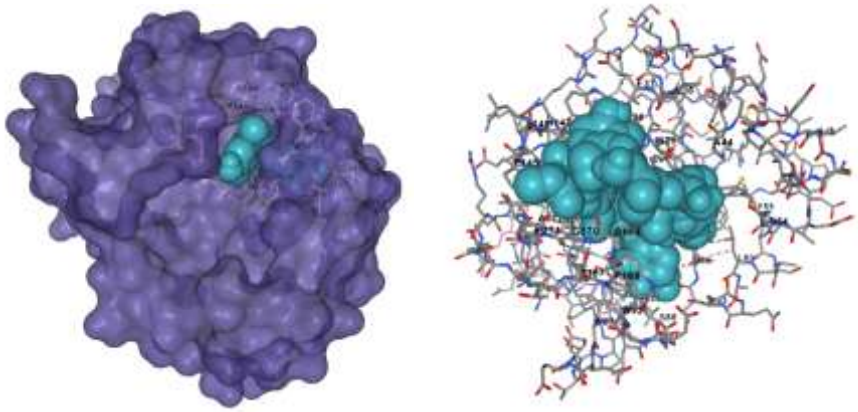

Figure 12: (a) Docked figure of Sappanchalcone with 2QIR (b) Docked figure of Sappanchalcone in conjugation with chitosan with 2QIR

Table 7: Docking scores for Sappanchalcone with and without Chitosan

CurPocket ID	Vina Score (Without Chitosan)	Vina Score (With Chitosan)	Cavity Volume (Å³)	Center (x, y, z)	Docking Size (x, y, z)
C1	-8.4	-8.1	771	3, 9, -20	22, 22, 22(without) / 39,39,39
C3	-8.0	-11.4	153	14, 17, -12	22, 22, 22(without) / 39,39,39
C5	-8.0	-12.7	65	13, 7, -13	22, 22, 22(without) / 39,39,39
C4	-6.8	-11.4	123	22, 12, -17	22, 22, 22(without) / 39,39,39
C2	-5.4	-9.5	712	10, 15, -34	22, 22, 22(without) / 39,39,39

Pocket C5 had the most notable increase in binding affinity (-12.7 with Chitosan vs. -8.0 without). The docking size was increased to **39, 39, 39** with Chitosan. Chitosan generally enhanced the binding affinity for all pockets.

Table 8: Interacting Residues for Sappanchalcone

Pocket	Score	Residues (Chain A)
C1(without chitosan)	-8.4	HIS34, ILE35, TRP38, TRP39, TRP92, ILE104, ASP105, GLN106, LEU107, LEU108, ALA109, GLN113, LEU114, GLY115, LYS116, GLY117, LEU118, GLY119, THR120, LEU122, THR141, ASP142, PRO143, SER144, ASN147, ARG149, ALA150, CYS153, TYR154, LYS156, ASP169
C5 (with chitosan)	-12.7	LEU30, HIS34, ILE35, VAL36, GLU37, TRP38, TRP39, ALA44, ARG45, PRO46, GLU53, GLN54, TYR55, VAL59, LEU60, GLU63, VAL65, GLN81, TYR83, VAL84, GLY87, SER88, GLY89, ASP90, TRP92, TRP93, ILE104, ASP105, GLN106, LEU107, LEU108, THR141, ASP142, PRO143, SER144, PRO145, SER146, ASN147, ARG149, ALA150, ILE151, CYS153, TYR154, THR167, PRO168, ASP169, GLY170, PRO171, ALA172

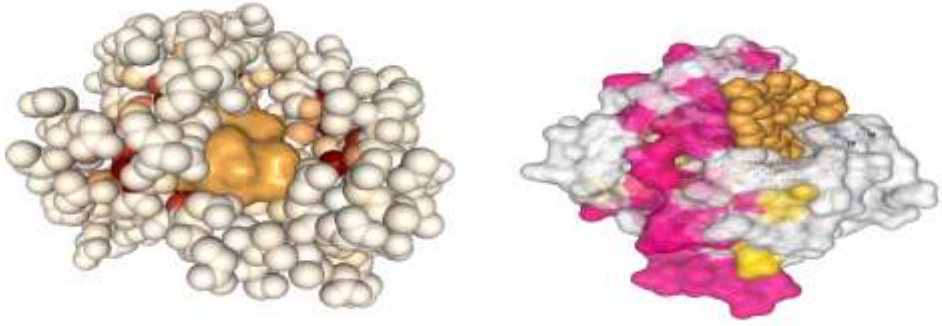

Figure 13: (a) Docked figure of Caesalpinin with 2QIR (b) Docked figure of Caesalpinin in conjugation with chitosan with 2QIR

Table 9: Docking scores for Caesalpinin with and without Chitosan

CurPocket ID	Vina Score (Without Chitosan)	Vina Score (With Chitosan)	Cavity Volume (Å³)	Center (x, y, z)	Docking Size (x, y, z)
C1	-4.8	-11.8	771	3, 9, -20	21, 21, 21(without) / 41, 41, 41
C3	-10.0	-10.4	153	14, 17, -12	21, 21, 21(without) / 41, 41, 41
C5	-9.3	-10.3	65	13, 7, -13	21, 21, 21(without) / 41, 41, 41
C4	-6.7	-9.4	123	22, 12, -17	21, 21, 21(without) / 41, 41, 41
C2	-5.5	-8.0	712	10, 15, -34	21, 21, 21(without) / 41, 41, 41

The docking scores improved significantly when Chitosan was used, indicating stronger binding. The best docking score without Chitosan was **-10.0 (C3)**, while with Chitosan, the best score improved to **-11.8 (C1)**. Chitosan-modified docking showed better interactions, with a general trend of lower (better) Vina scores.

Table 10: Interacting Residues for Caesalpinin

Pocket ID	Score	Residues in Chain A
C3 (without chitosan)	-10.0	TRP38, TRP39, ALA44, GLN54, TYR55, VAL59, LEU60, GLU63, VAL65, TYR79, GLN81, TYR83, VAL84, GLY87, SER88, GLY89, ASP90, TRP92, TRP93, ASP105, ASP142, PRO143, ASP169
C1(with chitosan)	-11.8	LEU30, SER33, HIS34, VAL36, GLU37, TRP38, TRP39, ALA44, ARG45, PRO46, ASP50, GLN54, TYR55, LEU60, GLU63, VAL65, TYR79, GLN81, TYR83, SER88, GLY89, ASP90, TRP92, TRP93, ILE104, ASP105, GLN106, GLY115, LYS116, GLY117, LEU118, GLY119, THR120, ASP142, PRO143, SER144, PRO145, SER146, ASN147, LEU148, ARG149, ALA150, ILE151, ARG152, CYS153, TYR154, LYS156, ARG161, THR164, THR167, PRO168, ASP169, GLY170, PRO171, ALA172, VAL173

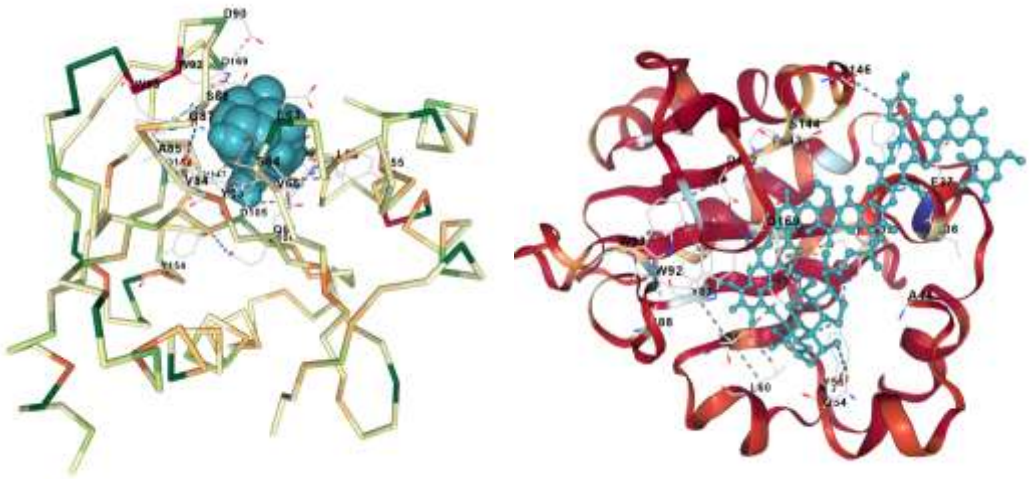

Figure 14: (a) Docked figure of Cholic Acid with 2QIR (b) Docked figure of Cholic Acid in conjugation with chitosan with 2QIR

Table 11: Docking scores for Cholic Acid with and without Chitosan

CurPocket ID	Vina Score (Without Chitosan)	Vina Score (With Chitosan)	Cavity Volume (Å³)	Center (x, y, z)	Docking Size (x, y, z)
C3	-9.3	-12.3	153	14, 17, -12	22, 22, 22(without) /38, 38, 38
C5	-8.2	-14.3	65	13, 7, -13	22, 22, 22(without) /38, 38, 38

C1	-8.0	-14.7	771	3, 9, -20	22, 22, 22(without) /38, 38, 38
C4	-7.2	-11.5	123	22, 12, -17	22, 22, 22(without) /38, 38, 38
C2	-5.7	-12.6	712	10, 15, -34	22, 22, 22(without) /38, 38, 38

Cholic acid was docked with the 2QIR protein both with and without chitosan. The results indicate that the presence of chitosan significantly improves the binding affinity, as shown by the more negative vina scores. Without chitosan, the best docking score was **-9.3** (CurPocket C3). With chitosan, the best docking score improved significantly to **-14.7** (CurPocket C1). Overall, the addition of chitosan enhanced the binding affinity across all pockets, with docking scores becoming more negative in all cases.

Table 12: Interacting Residues for Cholic Acid

Pocket	Score	Chain A Residues
C3 (without chitosan)	-9.3	LEU30, TRP38, TRP39, ALA44, PRO46, GLN54, TYR55, VAL59, LEU60, GLU63, SER64, VAL65, GLN81, TYR83, VAL84, ALA85, GLY87, SER88, GLY89, ASP90, TRP92, TRP93, ILE104, ASP105, GLN106, ASP142, PRO143, SER144, ASN147, TYR154, ASP169
C1 (with chitosan)	-14.7	SER33, HIS34, VAL36, GLU37, TRP38, TRP39, ALA44, ARG45, GLN54, TYR55, LEU60, GLU63, VAL65, GLN81, TYR83, SER88, ASP90, TRP92, TRP93, ASP105, ALA111, SER112, LEU114, GLY115, LYS116, ASP142, PRO143, SER144, PRO145, SER146, ASN147, LEU148, ARG149, TYR154, PRO168, ASP169, PRO171

Table 13: Summary Table of Docking Scores for 2QIR with All 5 Ligands

Protein Name	Ligand Name	Best Docking Score (With Chitosan)	Best Docking Score (Without Chitosan)
2QIR	Brazilin	-11.1	-9.3
2QIR	Brazilein	-14.8	-9.1
2QIR	Sappanchalcone	-12.7	-8.4
2QIR	Caesalpinin	-11.8	-10.0
2QIR	Cholic Acid	-14.7	-9.3

Table clearly shows that **all ligands exhibit stronger binding (lower vina scores) in the presence of chitosan**, highlighting its potential as an enhancer for molecular interactions.

Given the limited research on bacterial communities in Chennai's lakes, our study provides a crucial baseline for future investigations. The presence of antibiotic-resistant pathogens in lake water highlights potential public health risks. The effectiveness of *Caesalpinia sappan* extracts and chitosan nanoparticles in molecular docking studies suggests promising avenues for bioremediation efforts. Further studies should focus on in vivo validation and large-scale applications.

CONCLUSION

This study underscores the need for continuous monitoring of pathogenic bacterial communities in Chennai's lakes. The identification of antibiotic-resistant bacteria and potential natural inhibitors opens new possibilities for mitigating environmental and health risks associated with contaminated water bodies.

In docking studies, among the tested compounds, Brazilein and Cholic Acid exhibited the highest binding affinities with chitosan, with docking scores of -14.8 and -14.7, respectively. This suggests that these ligands have the strongest interactions with the target protein when combined with chitosan. The improved docking results in the presence of chitosan highlight its potential role as a biocompatible enhancer for drug binding and delivery applications. These findings support the potential application of chitosan as an effective biopolymer for improving ligand binding in drug discovery and molecular docking **studies**. Future research should focus on validating these computational results through experimental assays, such as in vitro binding studies and molecular dynamics simulations, to further confirm the stability and effectiveness of these ligand-protein interactions.

REFERENCES

1. Velrajan, Mahalakshmi. (2018). A study on bacterial diversity undertaken at Madras Christian college.

2. Raveen, R., Chennakrishnan, C., & Stephen, A. (2008). Impact of pollution on the quality of water in three freshwater lakes of suburban Chennai. *Nature Environment and Pollution Technology*, *7*(1), 61.

3. Chennakrishnan, C., Stephen, A., Manju, T., & Raveen, R. (2008). Water quality status of three vulnerable freshwater lakes of Suburban Chennai, India. *Ind. J. Environ. Ecoplan*, *15*(3), 591-596.

4. Raji, P. K., & Abraham, M. (2018). Comparative study of water quality of different lakes in Chennai. *Rasayan Journal of Chemistry*, *11*, 828-833.
5. Thangamalathi, S., & Anuradha, V. (2018). Seasonal variations in physico–chemical parameters of seven different lakes In Chennai, Tamil Nadu, India. *IOSR Journal of Environmental Science, Toxicology and Food Technology*, *12*(9), 11-17.
6. Shahina, S. J., Sandhiya, D., & Rafiq, S. (2020). Bacteriological quality assessment of groundwater and surface water in Chennai. *Nature Environment and Pollution Technology*, *19*(1), 349-353.
7. S. Karthick Raja Namasivayam, A.L. Francis, R.S. Arvind Bharani, C.Valli Nachiyar, Bacterial biofilm or biofouling networks with numerous resilience factors from real water supplies of Chennai and their enhanced susceptibility to biocompatible nanoparticles, Journal of Cleaner Production, Volume 231, 2019, Pages 872-898, ISSN 0959-6526, https://doi.org/10.1016/j.jclepro.2019.05.199.
8. Guentzel MN. Escherichia, Klebsiella, Enterobacter, Serratia, Citrobacter, and Proteus. In: Baron S, editor. Medical Microbiology. 4th edition. Galveston (TX): University of Texas Medical Branch at Galveston; 1996. Chapter 26. Available from: https://www.ncbi.nlm.nih.gov/books/NBK8035/
9. van Hoek, A. H., Mevius, D., Guerra, B., Mullany, P., Roberts, A. P., & Aarts, H. J. (2011). Acquired antibiotic resistance genes: an overview. *Frontiers in microbiology*, *2*, 203. https://doi.org/10.3389/fmicb.2011.00203
10. McKinney, W. (2012). *Python for data analysis: Data wrangling with Pandas, NumPy, and IPython*. " O'Reilly Media, Inc.".
11. McKinney, W. (2022). *Python for data analysis*. " O'Reilly Media, Inc.".
12. Liu, Y., Yang, X., Gan, J., Chen, S., Xiao, Z. X., & Cao, Y. (2022). CB-Dock2: improved protein-ligand blind docking by integrating cavity detection, docking and homologous template fitting. *Nucleic acids research*, *50*(W1), W159–W164. https://doi.org/10.1093/nar/gkac394
13. Gaurav verma, Uma kumari, AnbuMegala Murugesan, In-silico drug design in human apoptosis inducing factor (AIF) in lung cancer, Journal of emerging technologies and innovative research (JETIR), ISSN: 2349-5162, feb 2025, volume 12, issue 2
14. Aditi dwivedi, Uma kumari, AnbuMegala Murugesan, In-silico approach for potential drug target in human mutant complex with NADPH and AG-881 inhibitor, Journal of emerging technologies and innovative research (JETIR), ISSN: 2349-5162, feb 2025, volume 12, issue 2
15. McKinney, W. (2011). pandas: a foundational Python library for data analysis and statistics. *Python for high performance and scientific computing*, *14*(9), 1-9.
16. Sahoo, K., Samal, A. K., Pramanik, J., & Pani, S. K. (2019). Exploratory data analysis using Python. *International Journal of Innovative Technology and Exploring Engineering*, *8*(12), 4727-4735.
17. Sial, A. H., Rashdi, S. Y. S., & Khan, A. H. (2021). Comparative analysis of data visualization libraries Matplotlib and Seaborn in Python. *International Journal*, *10*(1), 277-281.
18. Nelli, F. (2015). *Python data analytics: Data analysis and science using PANDAs, Matplotlib and the Python Programming Language*. Apress.
19. Yuan, S., Chan, H. S., & Hu, Z. (2017). Using PyMOL as a platform for computational drug design. *Wiley Interdisciplinary Reviews: Computational Molecular Science*, *7*(2), e1298.
20. DeLano, W. L. (2002). Pymol: An open-source molecular graphics tool. *CCP4 Newsl. Protein Crystallogr*, *40*(1), 82-92.